

Pair production, Comptonization and dynamics in astrophysical plasmas

Paul W. Guilbert *Max-Planck-Institut für Extraterrestrische Physik, Garching.*

Susan Stepney *Institute of Astronomy, Cambridge*

Summary. Electron-positron pair production is an important cooling mechanism for plasmas at mildly relativistic temperatures. A thorough understanding of the process is necessary to explain the hard X-ray spectra of AGNs and gamma-ray bursters. We investigate thermal plasmas with temperatures $kT \approx m_e c^2$ and optical depths $1 \lesssim \tau \lesssim 5$, including pair processes, Comptonization and bremsstrahlung. Results are presented for equilibrium and impulsively heated models. We find that, in the former case, the observed spectrum is featureless, but in the latter case it can show a broad, flat annihilation feature. We then discuss non-thermal pair production in plasmas confined by strong magnetic fields, such as those thought to exist at the surface of neutron stars. We show that two photon pair production cannot give an annihilation feature, but that magnetic pair production ($\gamma B \rightarrow e^+ e^-$) can give a significant annihilation line. Finally we consider simple dynamical systems and the effect of expansion on the spectrum of a gas in which pair production is important. Adiabatic cooling steepens the flat spectral feature to ω^{-3} in the thermal case, and in the non-thermal case the spectrum has a flat component with a turnover at ~ 2 MeV.

1. Introduction

The observational evidence for the presence of electron-positron pairs is growing. An annihilation line has been observed from the galactic centre (Johnson, Harnden & Haymes 1972; Leventhal, MacCullam & Stang 1978). Several γ -ray bursts have a 400–500 keV feature which is probably an annihilation line (Mazets *et al.* 1982), and Cygnus X-1 may also show one (Nolan & Matteson 1983).

Pair production is also expected to be important in active galactic nuclei and galactic black hole sources, if the primary radiation mechanism produces more than 1 per cent of an Eddington luminosity above 1 MeV (Guilbert, Fabian & Rees 1983).

Pairs increase the cooling rate and the opacity of the source. They also affect the radiation transport, since annihilation acts as a hard photon source, and production as a photon sink. So, to interpret the observed hard spectra of active galactic nuclei, γ -ray bursters and other high-luminosity, compact sources, we need to understand the details of pair production and radiative transfer in very hot plasmas.

Progress has already been made on this front. Various accounts of time-scales, radiation processes and pair equilibria exist (see, for example, Lightman & Band 1981; Zdziarski 1982, 1984b; Lightman 1982; Stepney 1983a,b; and references therein). In particular, Svensson (1982, 1984) has made a detailed analytic study of constant temperature plasmas. Zdziarski (1984a) uses a Monte Carlo computer simulation, suitable for steady-state, homogeneous plasmas.

In this paper we discuss the case of moderate optical depth plasmas, $\tau \gtrsim 1$, where Comptonization is an important source of hard photons. We present an analytical discussion of both constant temperature (Section 2) and impulsively heated (Section 3) plasmas. In Section 4 we describe the results of a computer program developed to model inhomogeneous plasmas in a fully time-dependent manner. Section 5 contains a discussion of non-thermal pair production, and in Section 6 we consider the effects of dynamics, in both the thermal and

non-thermal case. Throughout this paper the terms ‘thermal’ and ‘non-thermal’ refer to the electron distribution, either Maxwellian or (for example) a power law, respectively.

We have found it convenient to work with dimensionless units in which energies and temperatures are expressed in terms of the electron rest mass, a natural unit for the problem under consideration. So a photon of energy $\omega = 1$ has a physical energy of 511 keV, and a particle temperature of $T = 1$ corresponds to a physical temperature of $T_* = 5.9 \times 10^9$ K.

It is also convenient to parameterize the gas by the so-called ‘proton optical depth’, $\tau_p = N_p \sigma_T R$, where N_p is the proton number density, σ_T is the Thomson cross-section, and R is the physical size of the system. This is a better choice than the true electron scattering optical depth, since the latter is a function of both the pair density (which can vary) and the photon energy (due to Klein-Nishina corrections to the cross-section).

A natural unit of time, then, is the ‘proton Thomson time’, $t_p = 1/N_p \sigma_T c = R/c\tau_p$. In physical units this becomes $t_p = 5000 \times (N_p/10^{16} \text{ m}^{-3}) \text{ s}$. z is used throughout as the ratio of pairs to protons.

2. Constant temperature plasmas

2.1 Preamble

For a plasma with given optical depth and temperature, what is the equilibrium pair density? The answer for an optically thick plasma, emitting like a blackbody, follows purely from thermodynamics. In the high temperature limit ($T \gg 1$) the pair density approaches three quarters of the blackbody photon density (the factor is different since electrons are fermions and photons are bosons). We are not interested in such enormous equilibrium pair densities here ($N_{e^+} \sim 10^{36} \text{ m}^{-3}$ at $T = 1$), since no astrophysical object radiates like a blackbody at these temperatures (flux $\sim 10^{32} T^4 \text{ W m}^{-2}$); the energy requirements are too great.

For plasmas with moderate optical depths the pair density must be calculated by considering the individual particle reactions. Lightman (1982) has coined the term ‘effectively thin’ to describe plasmas that are thin to photon absorptions, but not necessarily to photon scattering. These are the plasmas we shall be discussing.

In a truly thin plasma all photons escape without interacting, and only particle-particle interactions need be considered. In this case balancing production and annihilation rates gives a maximum temperature. Bisnovatyi-Kogan, Zel’dovich & Sunyaev (1971) first pointed out the existence of a maximum temperature, due to the production cross-sections increasing with temperature and the annihilation cross-section falling. They found $T_{max} = 40$. A more accurate determination of the rates (Svensson 1982; Stepney 1983b) gives $T_{max} = 24$.

Svensson (1982) considered in detail a plasma which is thin to scattering (that is the photons are not Comptonized), but not so thin that pair production by photons can be neglected. He discovered that, at a given temperature, there is a critical optical depth above which there are no equilibrium solutions, and below which there are two; one low- z branch stable to isothermal perturbations) and one high- z branch (unstable). Note that since the high- z branch can be stable to perturbations at constant heating, it may be physically obtainable. Isothermal models are computationally convenient, but unlikely in practice.

2.2 Comptonization

The other limit where it is possible to make progress analytically is when the optical depth is high enough that the emergent photon spectrum is significantly modified by Comptonization. In this case we can approximate the photon distribution by saying that all the bremsstrahlung photons with $\omega > \omega_{min}$ are Comptonized up to an energy $\omega \sim T$ before they escape. (For a

discussion of ω_{\min} see later.) Also they will not produce pairs until $\omega \sim 1$, since they will not be energetic enough.

In equilibrium, pair production balances annihilation. We make the further approximation that photon escape balances the production of hard photons via Comptonization of the internally-produced soft bremsstrahlung photons, that is, we neglect the annihilation photons. Annihilation photons are produced by pairs which must initially (perhaps many productions and annihilations ago) have been produced by Comptonized bremsstrahlung (Cb) photons. If the annihilation photons produce pairs, nothing has changed. If they escape, it is equivalent to the escape of the original Cb photons.

This argument breaks down if the temperature is so low that the annihilation photon gets down-scattered from $\omega \sim 1+T$ (where it is produced) below the pair production threshold before it has time to make another pair. Since the hard $\omega \sim 1+T$ photon preferentially interacts with a soft $\omega \sim 1/1+T \sim 1-T$ photon (thus maximizing the cross-section) the criterion is that there be enough soft bremsstrahlung photons of this energy, i.e. that $T \gtrsim 1-T, T \gtrsim 0.5$.

So, provided that $kT_* \gtrsim m_e c^2/2$, we can neglect the annihilation photons in this approximation. (Of course, in a detailed numerical calculation the annihilation photons must be included properly.)

2.3 Low Energy Cut-Off

There are two competing processes that determine ω_{\min} , the energy below which bremsstrahlung photons can be ignored. The first is that the photons scatter up to $\omega \sim T$ before escaping. For soft photons ($\omega \ll T$) at temperatures $T \sim 1$ the relative energy shift per scattering is roughly a factor of 10 (Guilbert 1981b). So a photon which starts with energy ω_0 has an energy $\omega \sim \omega_0 \times 10^n$ after n scatterings, provided $\omega < T$. The average number of scatterings a photon undergoes before escape is $n_{esc} \sim \tau_{es}^2$. So the conditions for ω_{\min}^c becomes

$$\begin{aligned} T &\sim \omega_{\min}^c \times 10^{n_{esc}} \\ \omega_{\min}^c &\sim T \times 10^{-\tau_{es}^2} \end{aligned} \quad (1)$$

The second process, more important at higher optical depths ($\tau > 3$) is bremsstrahlung self-absorption. (That the very soft bremsstrahlung photons are self-absorbed does not alter the fact that the plasma is ‘effectively thin’, since the hard, $\omega \sim 1$, photons involved in pair production are not self-absorbed.)

The blackbody flux in the Rayleigh-Jeans limit is

$$\begin{aligned} B_v^{RJ} &= 8\pi\nu^2 kT_*/c^2 \quad \text{W m}^{-2} \text{ Hz}^{-1} \\ \frac{dE^{RJ}(\omega)}{dt} &= \frac{\omega^2 T}{\pi^2} \left(\frac{\alpha_f}{r_e} \right)^3 \frac{1}{\tau_p N_p} \end{aligned} \quad (2)$$

The units in equation (2) are $m_e c^2$ per proton per Thomson time per $m_e c^2$. In the same units the soft bremsstrahlung emission is (to within factors of 2, and neglecting logarithmic factors)

$$\frac{dE^{soft}(\omega)}{dt} \simeq \begin{cases} 10\alpha_f (T^{1/2} + 1/T^{1/2}); & T < 1 \\ 20\alpha_f; & 1 < T \end{cases} \quad (3)$$

where the $T^{1/2}$ term represents electron-electron bremsstrahlung, and the $1/T^{1/2}$ term, the electron-proton bremsstrahlung. These fluxes are equal at an energy of ω_{\min}^{ff} :

$$\omega_{\min}^{ff} = \pi \sqrt{\left(\frac{r_e}{\alpha_f}\right)^3 \frac{\tau_p N_p}{T} \frac{dE^{soft}(\omega)}{dt}} \quad (4)$$

At $T \sim 1$, if $N_p \tau_p \sim 10^{16} \text{ m}^{-3}$, then $\omega_{\min}^{ff} \sim 3 \times 10^{-11}$ and if $N_p \tau_p \sim 10^{24} \text{ m}^{-3}$, then $\omega_{\min}^{ff} \sim 3 \times 10^{-7}$.

So the value of ω below which the bremsstrahlung photons can be neglected is

$$\omega_{\min} = \max(\omega_{\min}^c, \omega_{\min}^{ff}) \quad (5)$$

If we approximate the bremsstrahlung spectrum by

$$\frac{dN^{ff}(\omega)}{dt} \sim \begin{cases} 0; & \omega < \omega_{\min} \\ \frac{1}{\omega} \frac{dE^{soft}(\omega)}{dt}; & \omega_{\min} < \omega < T \\ 0; & T < \omega \end{cases} \quad (6)$$

then the number of bremsstrahlung photons produced per proton per Thomson time is

$$\frac{dn^{ff}(\omega)}{dt} = \int_{\omega_{\min}}^T \frac{1}{\omega} \frac{dE^{soft}(\omega)}{dt} d\omega = \frac{dE^{soft}}{dt} \ln(T/\omega_{\min}) \quad (7)$$

and these are Comptonized up to an energy $\omega \sim T$. Thus equation (7) gives the number of Cb photons produced per proton per Thomson time (including the contribution of pairs) as

$$\frac{dn^{Cb}}{dt} \simeq (1+2z)^2 N^{Cb} \quad (8)$$

where

$$N^{Cb} = \begin{cases} 10\alpha_f (T^{1/2} + 1/T^{1/2}) \ln(T/\omega_{\min}); & T < 1 \\ 20\alpha_f \ln(T/\omega_{\min}); & 1 < T \end{cases}$$

$N^{Cb} \sim 2$ for $T = 1$, $\omega_{\min} = 10^{-7}$. It is only a weak function of ω_{\min} and T for $T > 1$, and goes as $T^{-1/2}$ for $T < 1$.

2.4 Photon Balance

We now balance photon escape with the production of hard Cb photons given by equation (8). The photon escape time (in proton Thomson times) is

$$t^{esc} \simeq \tau_{es}^2 (\tau_p / \tau_{es}) = (1+2z)\tau_p^2 \quad (9)$$

So the photon balance becomes

$$\frac{dn}{dt} = (1+2z)^2 N^{Cb} - \frac{n}{(1+2z)\tau_p^2} = 0 \quad (10)$$

The pair production and annihilation rates (neglecting annihilation photons) are

$$\frac{dz^{prod}}{dt} \simeq [n \exp(-1/T)]^2; \quad \frac{dz^{ann}}{dt} \simeq \frac{z(1+z)}{1+T^2} \quad (11)$$

The factor of $\exp(-1/T)$ gives the exponential cut-off in the photon-photon rate at low temperatures (below threshold). The factor of $1/(1+T^2)$ gives the correct low and high temperature limits of the annihilation rate. Balancing these rates gives

$$n^2 = \frac{\exp(2/T)}{1+T^2} z(1+z) \quad (12)$$

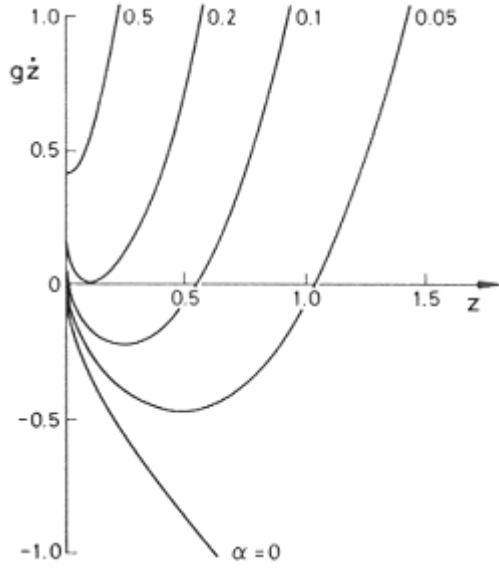


Figure 1. The pair production rate, $g \dot{z}$, as a function of the pair density z , labelled by different values of the parameter $a \propto \tau_p^2$. Below the critical value ($a_{crit} \approx 0.2$) there are two solutions to $z = 0$. The high- z solution is unstable (the slope of z is positive). Above the critical value there are no solutions.

Substituting for n in equation (10) gives

$$g \frac{dz}{dt} = a(1+2z)^3 - \sqrt{z(1+z)} = 0 \quad (13)$$

where

$$g(z, \tau_p) = \frac{\tau_p^2 (1+2z)^2}{2\sqrt{z(1+z)}}$$

and

$$a = N^{Cb} \tau_p^2 \exp(-1/T) \sqrt{1+T^2}$$

Solutions of this equation (which is essentially $dz/dt = 0$) give the equilibrium values of the pair density, z , and depend on the parameter $a(T, \tau_p)$. Fig. (1) shows $g dz/dt$ plotted as a function of z for different values of a . For some high values of a there are no equilibrium solutions. For low values of a there are two. These are the high optical depth analogues of the two solutions found by Svensson (1982). Again, the high- z solution is unstable (the slope of z is positive). The critical value of a for which there is only one solution occurs when $d\dot{z}/dz = 0$ at $\dot{z} = 0$. This can be found by differentiating equation (13) with respect to z . We find $z_{crit} \approx 0.1$, $a_{crit} \approx 0.2$. Hence the criterion for an equilibrium solution to exist is

$$a < a_{crit} \approx 0.2$$

$$\Rightarrow \tau_p < \frac{0.4}{\sqrt{N^{Cb}}} \frac{\exp(2/T)}{(1+T^2)^{1/4}} \quad (12)$$

This is shown in Fig. (2), along with the equilibrium values of z in the stable region. The actual values of $T_{crit}(\tau_p)$ should not be taken too seriously, since we have been neglecting factors of order 2 throughout. The functional dependence, however, is real. To get more accurate values of T_{crit} , we will use a numerical method, described in Section 4. Svensson (1984) also discusses this in more detail.

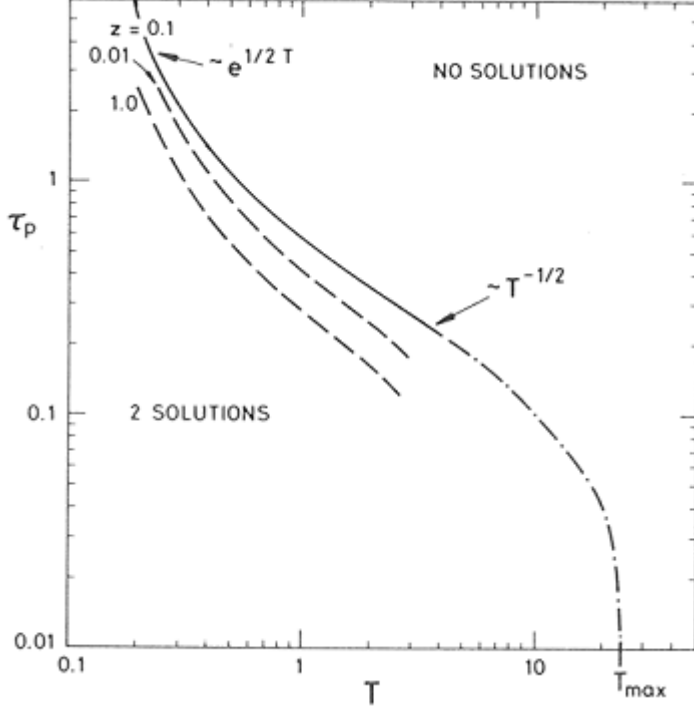


Figure 2. The T , τ_p plane showing the division between the region with two equilibrium solutions, and that with none (see equation 14). Lines of constant z are labelled. The dash-dot curve shows a smooth interpolation between the zero optical depth limit ($T_{max} = 24$) and the work of this paper.

3. Impulsively heated plasmas

The constant temperature case is the simplest to analyse, since it only depends on two parameters, T_e and τ_p , and energy balance need not be considered. The next simplest case is an impulsively heated gas which is then allowed to cool freely. We assume that the protons are effectively ‘instantly’ heated (i.e. on a time-scale very much shorter than any other relevant time-scale) to a temperature of a few tens of $m_e c^2$. They then heat the electrons (we assume by Coulomb interaction) which are Compton-cooled by their own bremsstrahlung. Pairs are produced in the process. How efficiently is the large initial thermal energy of the protons converted into pairs?

Fortunately this problem also turns out to depend on only two parameters (to within the accuracy of our assumptions), this time T_p and τ_p . But now energy balance must be included. The model does not depend on the initial electron temperature, T_e^{init} . Instead, this is determined by saying that the protons rapidly heat the electrons until Compton cooling balances Coulomb heating.

The production rate of Comptonized bremsstrahlung photons is given by equation (8), and these all receive an energy T_e . So the Compton cooling rate is just

$$\frac{dE^{cool}}{dt} \approx T_e N^{Cb} (1 + 2z)^2 \quad (15)$$

This is the change in the thermal energy of the electrons per proton. To get the thermal energy per electron (as required to calculate the electron temperature) divide by $1 + 2z$.

The Coulomb heating is

$$\frac{dE^{heat}}{dt} \approx h(T_p - T_e)(1 + 2z) \frac{1 + T_e^{1/2}}{T_e^{3/2}} \quad (15)$$

where $h \equiv (3m_e/2m_p) \ln \Lambda \approx 10^{-2}$ for a Coulomb logarithm $\ln \Lambda = 20$ and the factor of $(1 + T_e^{1/2})/T_e^{3/2}$ gives the correct high and low temperature limits (Stepney & Guilbert 1983).

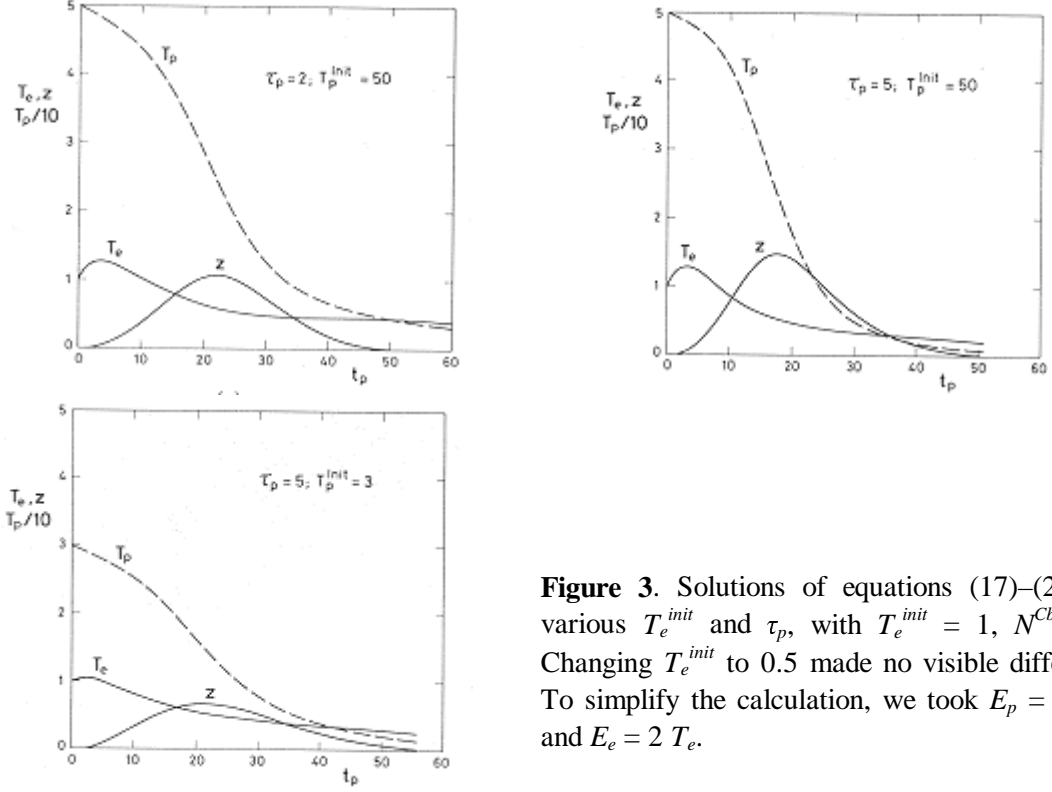


Figure 3. Solutions of equations (17)–(20) for various T_e^{init} and τ_p , with $T_e^{init} = 1$, $N^{Cb} = 0.5$. Changing T_e^{init} to 0.5 made no visible difference. To simplify the calculation, we took $E_p = 3 T_p/2$ and $E_e = 2 T_e$.

Putting $z = 0$ (as we assume there are no pairs initially) and balancing these rates gives the maximum electron temperature as a function of the initial proton temperature. For $N/h = 100$ and $T_e^{init} \sim 1$, this relation is reasonably well fitted by $T_e^{init} \simeq 0.2\sqrt{T_p^{init}}$. So an initial proton temperature of a few tens of $m_e c^2$ can support a maximum electron temperature of about an $m_e c^2$.

To get the time dependence, and to find the maximum pair density, z_{max} , we have to solve simultaneously the four equations for pair production, photon production, and electron and proton energy balance:

$$\frac{dz}{dt} = [n \exp(-1/T_e)]^2 - \frac{z(1+z)}{1+T_e^2} \quad (17)$$

$$\frac{dn}{dt} = N^{Cb}(1+2z)^2 - \frac{n}{(1+2z)\tau_p^2} - 2\frac{dz}{dt} \quad (18)$$

$$\frac{dE_p}{dt} = -h(1+2z)(T_p - T_e) \frac{1+T_e^{1/2}}{T_e^{3/2}} \quad (19)$$

$$\frac{dE_e}{dt} = -\frac{dE_p}{dt} - T_e N^{Cb}(1+2z)^2 \quad (20)$$

Notice that now annihilation photons are included in the photon production rate, since we are not in equilibrium.

It is straightforward to solve these equations numerically – the results are shown in Fig. (3). The solutions are insensitive to T_e^{init} ; the electron temperature rapidly rises to $\sim T_e^{max}$ before many pairs are produced, due to the short Compton cooling and Coulomb heating time-scales. The dependence on T_p is strong, but indirect; a lower T_p results in a lower T_e^{max} , and so a lower pair production rate.

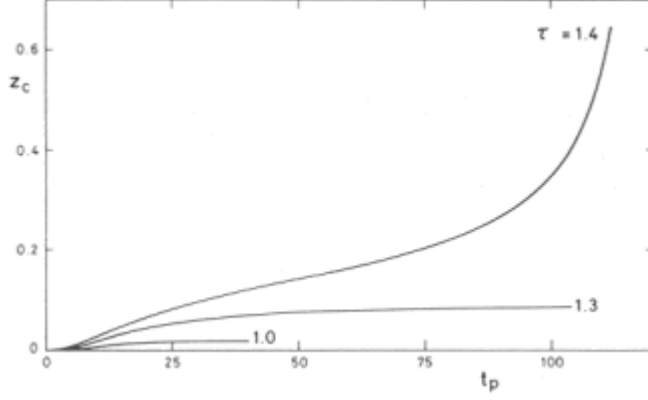


Figure 4. Central pair density against time for three constant-temperature computer models. All the models had $T = 1$, but different optical depths. They show the transition from convergent to runaway behaviour.

We can find an expression for z_{max} and $T_e(z_{max})$ by the following argument: assume that $z_{max} > 1$ and $T < 1$, then equation (17) gives the maximum pair density as

$$z_{max} \sim n \exp(-1/T_z) \quad ; \quad T_z \equiv T_e(z_{max}) \quad (21)$$

From conservation of energy, the maximum number of photons (with energy $\omega \sim T$) is

$$n_{max} \sim \left(\frac{3}{2} \Delta T_p - 2z_{max} \right) / T_z \quad (22)$$

where $\Delta T_p = T_p^{init} - T_p(z = z_{max}) \approx T_p^{init}$. This gives an upper limit to z_{max} of

$$z_{max} \lesssim \left(\frac{\frac{3}{2} T_p - 2z_{max}}{T_z} \right) \exp(-1/T_z) \quad (23)$$

$$\Rightarrow z_{max} \lesssim \frac{3}{2} T_p^{init} / [2 + T_z \exp(1/T_z)]$$

So the maximum possible value for z_{max} (putting $T_z = 1$) is $\sim T_p/3$. As can be seen from Fig. (4), $T_z < 1$, and so z_{max} is given by

$$z_{max} \lesssim 3 T_p^{init} \exp(-1/T_z) 2 T_z \quad (24)$$

z_{max} is thus very sensitive to T_z . The computer model (see later) indicates that $T_z \sim 0.2$ when $z = z_{max}$. So for $T_p^{init} = 50$,

$$z_{max} \lesssim 2 - 3 \quad (25)$$

The inaccuracies in this approximation, especially in estimating the number of photons above threshold with a crude $\exp(-1/T_e)$ factor, mean that z_{max} cannot be estimated accurately. However, we can reverse the equation to obtain $T_e(z_{max})$:

$$T_e(z_{max}) \approx 1 / \ln \left(\frac{3}{2} \frac{T_p^{init}}{T_e z_{max}} \right) \quad (26)$$

$$\approx 1 / \ln \left(\frac{3}{2} T_p^{init} \right)$$

Hence, if $T_p^{init} = 50$ then $T_e(z_{max}) \approx 0.2$, and if $T_p^{init} = 20$ then $T_e(z_{max}) \approx 0.3$, in good agreement with the computer results. In particular we can see that the *larger* T_p^{init} is, the *smaller* we expect $T_e(z_{max})$ to be. So the hotter the gas is initially, the cooler the emitted photons; the photon spectrum will indicate that the gas is colder when T_p^{init} is higher.

Since factors of ~ 2 have been neglected in deriving these results, again only the qualitative form of the results should be taken seriously. However, we do expect a maximum pair density of a few, after a few tens of Thomson times.

4. A more detailed model

As shown in the previous sections, it is possible to make some progress analytically, but as soon as detailed results are required, the problem rapidly becomes intractable. Even numerical modelling of time-dependent plasmas at mildly relativistic temperatures requires a new technique. Fokker-Planck methods are not valid since the energy changes per scattering are not small, but of the same order as the particle energies. Monte Carlo methods are not well suited to model time-dependence.

4.1 The Computer Model

The program we shall describe below was originally designed to investigate Comptonization of an external flux of soft photons by a high-temperature plasma. It has been described in more detail by Guilbert (1981a). It was structured in such a way that it proved (relatively) easy to add internal sources and sinks of photons, and pairs.

The model, which has slab geometry, includes the following processes:

- (1) Comptonization. This redistributes the photons in energy, and can be considered as a ‘source’ of hard photons.
- (2) Photon transport – spatial redistribution.
- (3) Thermal bremsstrahlung – a soft photon source.
- (4) Annihilation – a hard photon source.
- (5) Pair production – a hard photon sink.
- (6) Coulomb heating (where appropriate).

For a discussion of the reaction rates used, see Stepney & Guilbert (1983).

We assume the particles (electrons, positrons and protons) have thermal, isotropic (but not necessarily spatially homogeneous) distribution functions, the electrons and positrons having the same temperature. This temperature is calculated from the energy balance. The photons are binned in energy (using a logarithmic grid $\Delta\omega/\omega \propto T$) and angle, as well as spatially. The photon distribution is calculated self-consistently. Each timestep the photons are scattered in energy and angle, and transported spatially. The changes in photon number and pair density due to the various processes are found, and the appropriate bins incremented.

In equilibrium models, the spatial grid is set by the optical depth. Since we only consider one Compton scattering per photon per iteration, the grid must not be so coarse that it grossly underestimates the effect of multiple scatterings. Thus we require $\Delta\tau_{es} \lesssim 1/3$. In cooling models care must also be taken that the timestep is not too large, to ensure that, for example, $\Delta T_e \ll T_e$. Since in this model $\Delta t = \Delta\tau_p$ (simplifying photon transport) this also sets a limit on $\Delta\tau_p$. If there is no external photon source the slab is symmetric, so only one half needs to be modelled. For low optical depths and low z , this means that typically four or eight spatial bins are sufficient. For the impulsively heated plasmas, 32 or 64 bins are required around z_{max} . The program is adaptive, and adjusts the size of the spatial bins as necessary to maintain $\Delta\tau_{es} \lesssim 0.3$.

The number of angle bins must not be so small that all photons scatter into the same bin. Eight angle bins are usually sufficient, except when the photons are very hard, if $\omega \gg 1+T$, which could only occur if an external hard photon source was present.

The logarithmic energy grid ensures adequate resolutions at all energies. For temperatures $T \sim 1$ and photon energies $10^{-6} < \omega < 10$, typically 80 bins are sufficient. Even at lower temperatures photons with energies $\omega \sim 10$ must be permitted, to treat the hard annihilation photons properly.

The program was originally written to run on an IBM 370 or IBM 3081. However, it vectorizes efficiently, and so runs well on a CRAY.

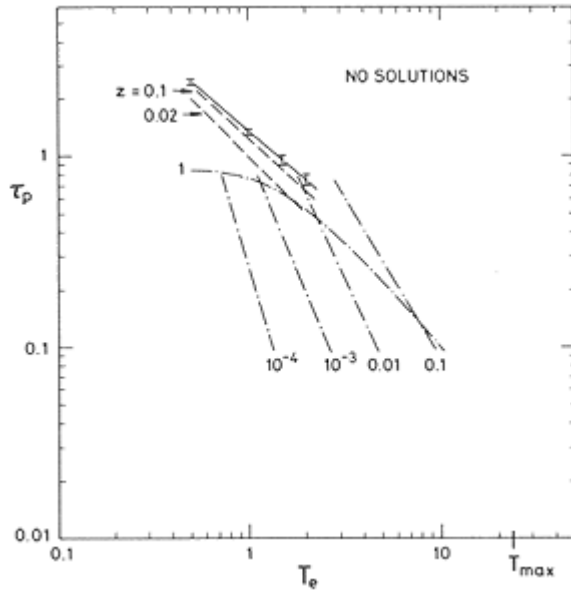


Figure 5. Computer results in the T, τ_p plane. The solid line divides the plane into two regions (cf. Fig. 2). The error bars indicate our exploration of parameter space – the model at the top of a bar diverged, the one at the bottom converged. The dash-dotted lines are adapted from Svensson (1982).

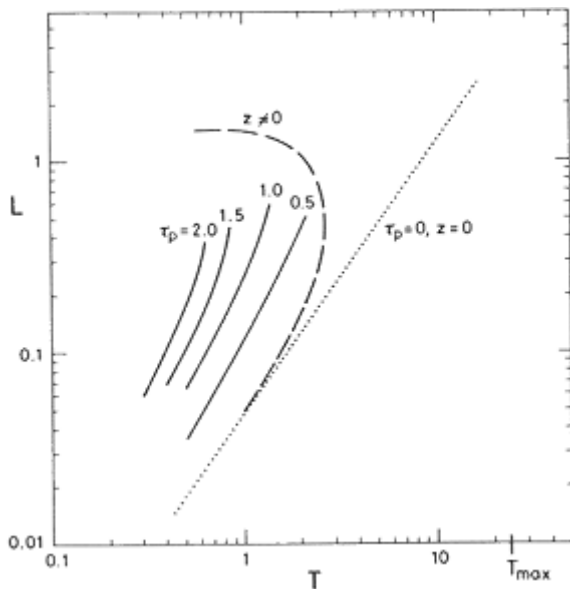


Figure 6. Output luminosity ($m_e c^2$ per proton per Thomson time) as a function of temperature and optical depth. The dotted line is pure bremsstrahlung emission from a $z = 0$ plasma. The dashed line is from Svensson (1982), which deviates from the bremsstrahlung line because the pair density is non-zero (increasing the bremsstrahlung and adding some annihilation photons). The solid lines are the computed results of this paper. Here z is quite low (< 0.1), and the deviations are mainly due to Comptonization of the soft bremsstrahlung photons.

4.2 Constant Temperature

To find the equilibrium solution, a model is held at a constant temperature; energy balance is not considered. Initially the model has no photons or pairs. It evolves until the pair density either converges to an equilibrium value, or diverges.

The results for a typical run are shown in Fig. (4). Since bremsstrahlung produces the soft photons being Comptonized, models take many Thomson times ($\gtrsim 137$) to converge. The regions of stable solutions are shown in Fig. (5), along with Svensson's (1982) low optical depth results. The boundary line here is slightly lower, as would be expected from the inclusion of Comptonization. Otherwise the results are in good agreement.

The luminosity as a function of temperature is shown in Fig. (6). The deviations from the $z = 0$ bremsstrahlung curve are large, even when z is low. This shows the effect of Compton upscattering the soft bremsstrahlung photons.

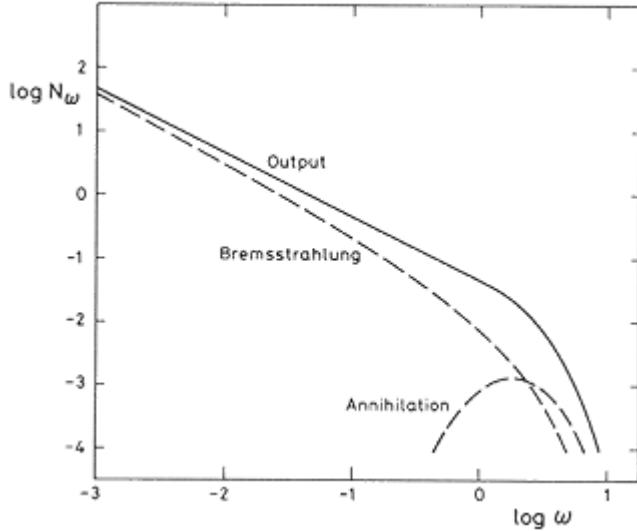


Figure 7. The output photon spectrum (photons per proton per Thomson time) from an equilibrium model ($T = 1$, $\tau_p = 1.2$) with the relevant bremsstrahlung and annihilation spectra for comparison.

The output spectrum of a typical model is shown in Fig. (7), along with an optically-thin bremsstrahlung and an annihilation spectrum for comparison. The result of Comptonization can be seen in the flatness of the spectrum, which is harder than the bremsstrahlung source. It is also harder than any observed γ -ray spectrum, as far as we are aware, and has no annihilation feature. To produce a more realistic spectrum one of the assumptions – steady state, isolated, thermal – must be relaxed. We shall first relax the steady state assumption.

4.3 Impulsive Heating

Physically, the unstable region in Fig. (2) represents catastrophic cooling by pair production. If a real plasma were initially to have a temperature and optical depth in this region it would rapidly cool. This is modelled by allowing the temperature of the electrons and protons to vary with time, and with position in the slab, by including energy balance. This extension causes the program to run at about half the speed of an equilibrium model since certain temperature-dependent rates (in particular Compton scattering) have to be recalculated each iteration. The central temperatures and pair densities as a function of time are shown, for various initial conditions, in Fig. (8).

The electron and proton temperatures and the central pair density vary in an identical manner to the solutions of the simplified equations derived earlier (equations 17–20). The spectra at early times, before much pair production has taken place, are simple Comptonized bremsstrahlung spectra. Hardly any energy escapes during this phase, however, since most of the proton cooling occurs when $z > 1$. Due to the large scattering depth when $z > 1$, not much radiation can escape until after the pairs have annihilated. So nearly all the energy escapes after the gas, protons and electrons, is cold. The instantaneous spectra at these late times look much like the time-averaged spectrum (see Fig. 9). There are three regions: a low-energy Comptonized bremsstrahlung spectrum $N(\omega) \propto \omega^{-1}$, a break to $N(\omega) \propto \text{constant}$, due to the down scattering of annihilation and the original hard bremsstrahlung photons, and an exponential turnover at a few kT_e .

Introducing an external flux of soft photons which dominates the soft bremsstrahlung photons does not change things a great deal (Fig. 10). In particular note that the value of T_e after cooling is unaffected, since this is determined by conservation of energy (Section 3) independent of the soft photon source. It does, however, speed up the availability of hard photons. The time-scale to reach z_{max} can therefore be greatly reduced. z_{max} itself is reduced,

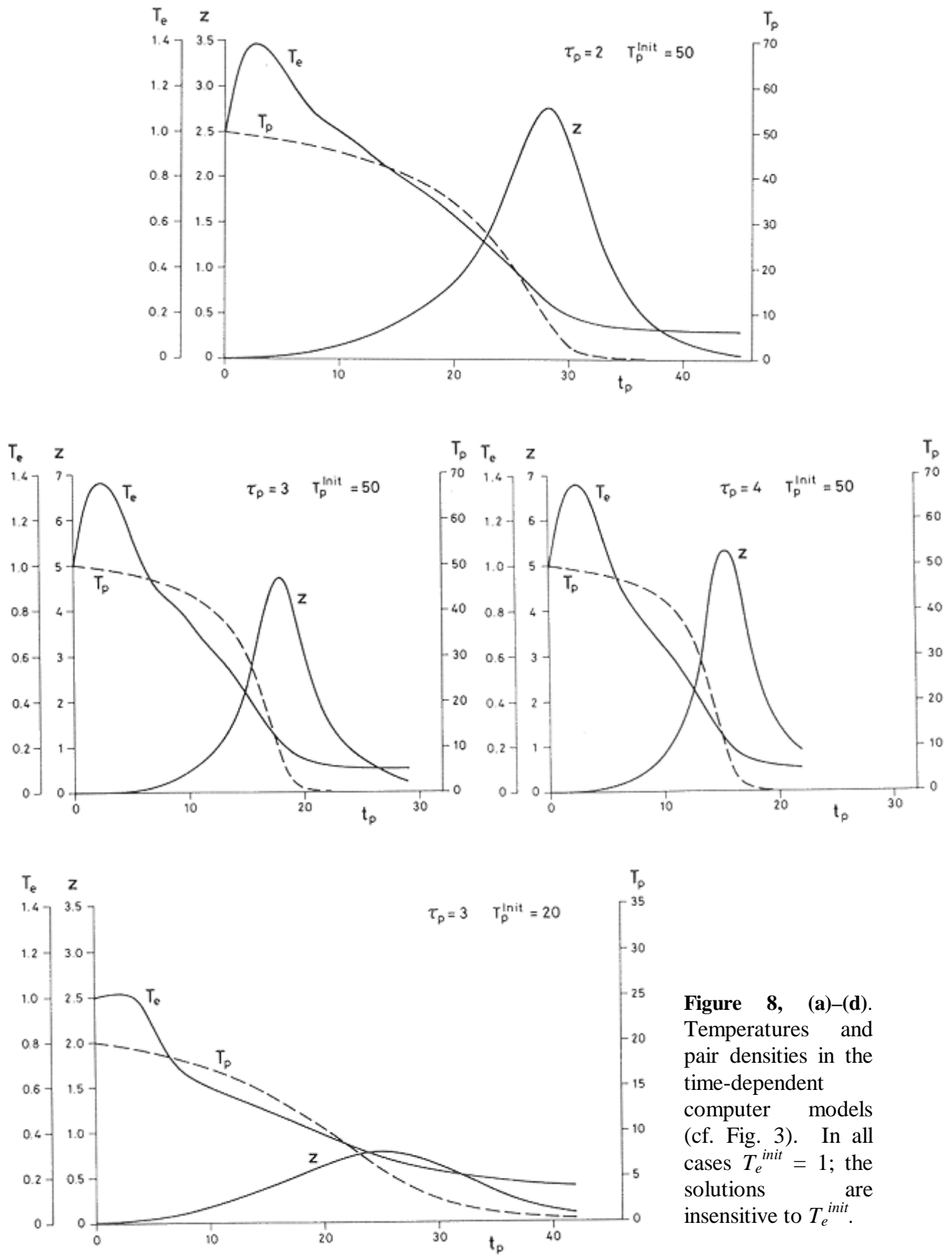


Figure 8, (a)–(d). Temperatures and pair densities in the time-dependent computer models (cf. Fig. 3). In all cases $T_e^{init} = 1$; the solutions are insensitive to T_e^{init} .

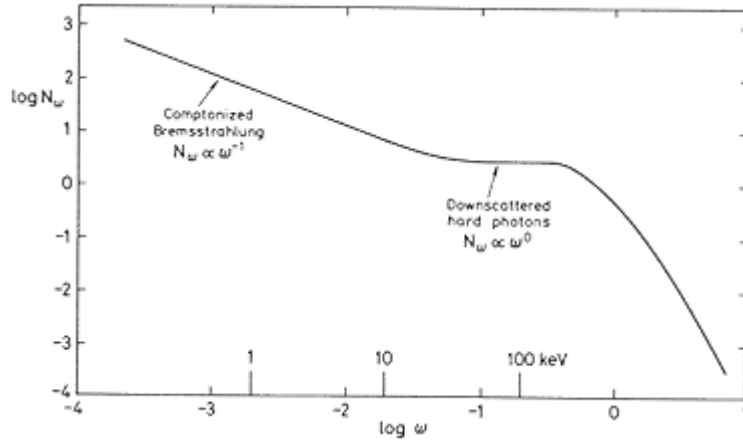


Figure 9. The time-averaged photon spectrum (photons per proton per Thomson time) from the model in Fig. 8 with $T_p^{init} = 50$, $\tau_p = 3$. The flat portion is from down-scattered annihilation and original hard bremsstrahlung photons.

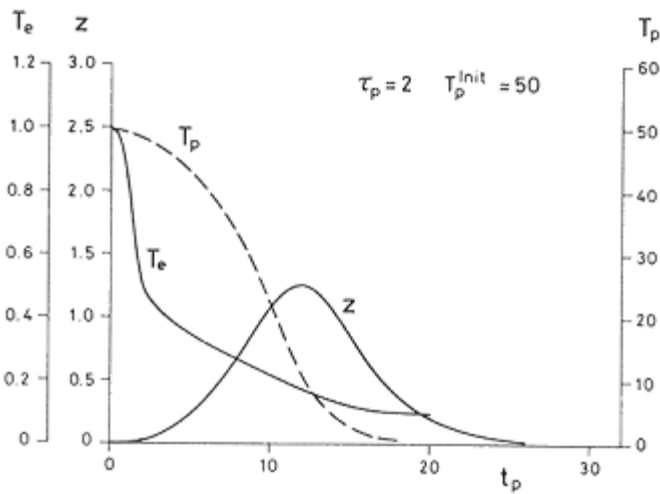


Figure 10. A time-dependent computer model having a central source of photons of luminosity $0.02 m_e c^2$ per proton per Thomson time, at an energy of $10^{-2} m_e c^2$. The model had $T_p^{init} = 50$, $\tau_p = 2$.

however, due to the increased Compton cooling and the consequent lower values of T_e at all times up to t_{cool} .

These thermal models seem unlikely to apply in astrophysical situations since the spectrum is much too hard. This is an inevitable feature of thermal models; bremsstrahlung has a very hard spectrum, which is made even harder by Comptonization. We note, however, that pair production in such plasmas greatly reduces the time needed to cool the protons (which contain all the energy initially). So the conclusion in Guilbert, Fabian & Stepney (1982) that some faster process than two-body electron-ion coupling may have to occur in certain highly variable sources is not necessarily correct.

5. Non-thermal pair production in confined plasmas

We have seen that it is very unlikely we shall ever observe a line feature from a thermal plasma; when the pairs are produced conditions are too hot and too optically thick. Guilbert, Fabian & Rees (1983) have also shown that line features are unlikely to be observed from unconfined non-thermal sources since if pair production is important then the Thomson depth is large.

In the case of the galactic centre source, the pair annihilation that produces the observed line is assumed to take place in a cold gas outside the production region (Bussard, Ramaty & Drachman 1979). Such a region is outside the scope of this work. The feature in γ -ray burst spectra may well come from the production region, however. If it is an annihilation line it is redshifted, and so presumably originates at the surface of the neutron star. Magnetic field strengths on the surface of neutron stars are high enough to confine a pair plasma, even when

the luminosity is more than sufficient to overcome gravity ($L \gg L_{Edd} / 2000$). They can also induce single-photon pair production. The field ensures that the pairs are cool. As we shall see below, an observable line feature may be produced from such a magnetically confined plasma. First, however, we consider ordinary two-photon pair production and show that, if this is the dominant mechanism, a narrow line feature is impossible.

5.1 Two-Photon Pair Production

Consider a source with dimensions $R^2 h$, $h \ll R$, and a spectrum

$$N(\omega) = \frac{L}{(\omega_M m_e c^2)^2} (2 - \alpha) \left(\frac{\omega}{\omega_M} \right)^{-\alpha} \begin{cases} \omega_0 < \omega < \omega_M \\ 1 < \alpha < 2 \\ \omega_0^{2-\alpha} \ll 1 \ll \omega_M^{2-\alpha} \end{cases} \quad (27)$$

where L is the luminosity. Assuming that only two-photon pair production ($\gamma + \gamma \rightarrow e^+ + e^-$) is important, an atmosphere with dimensions $h_{\gamma\gamma} R$ will be produced. Calculating the optical depth to pair production as a function of photon energy requires a numerical integration over the cross-section. However, we shall write

$$\tau_{\gamma\gamma}(\omega) \equiv a \sigma_T h_{\gamma\gamma} \int_{\sqrt{2}/\omega}^{\omega_M} \frac{N(\omega_1)}{R^2 c} \left(\frac{\sqrt{2}}{\omega \omega_1} \right) d\omega_1 m_e c^2 \quad (28)$$

where a is a function of the geometry and of ω_M . The maximum cross-section is less than σ_T and so for this choice of integrand, a is less than unity for any angular distribution of photons. The optical depth $\tau_{\gamma\gamma}$ is thus

$$\tau_{\gamma\gamma}(\omega) = \frac{l h_{\gamma\gamma}}{R} \frac{2 - \alpha}{\alpha} \frac{a}{\omega_M^{2-\alpha}} \left(\frac{\omega}{\sqrt{2}} \right)^{\alpha-1} \quad (29)$$

where $l \equiv L \sigma_T / R m_e c^2$ is a dimensionless luminosity such that if every $m_e c^2$ of photons were converted into an electron the Thomson length $N_e \sigma_T R$ would be l . If the pairs are to be confined (if the annihilation time-scale is shorter than the escape time-scale), then $\tau_{\gamma\gamma}(1) > 1$ for $h_{\gamma\gamma} < R$. Hence we require

$$l > \frac{\alpha}{2 - \alpha} \frac{\omega_M^{2-\alpha}}{a} \quad (30)$$

Now

$$l = 2\pi \frac{m_e}{m_p} \frac{R_S}{R} \frac{L}{L_{Edd}} \simeq 10^4 \frac{R_S}{R} \frac{L}{L_{Edd}} \quad (31)$$

where R_S is the Schwarzschild radius of the source. For a γ -ray burst at the surface of a neutron star the inequality (30) should not be difficult to satisfy, provided that ω_M is not too large and a is not too small (the source is not highly beamed). The Thomson depth of the pairs in equilibrium is then found to be

$$\tau_{es}^2 \simeq \frac{4x}{ab} \frac{\alpha}{\alpha - 1} \quad (32)$$

where the annihilation rate is $b \sigma_{TC}$, $b < 1$, and x is the average number of pairs produced per γ -ray photon, $x > 1$. So even for the minimum energy-to-pairs conversion efficiency, $x = 1$, the Thomson depth of the pairs is greater than one. Even if the source is highly beamed, if the inequality (30) is satisfied, then the value of a for an isotropic radiation field can be used in equations (29) and (32), since $\tau_{es} > 1$, and so Compton scattering will destroy the beaming.

5.2 Single-Photon Pair Production

Magnetic pair production involves the interaction of a single photon with a strong magnetic field (Erber 1966; Daugherty & Harding 1983). The threshold photon energy is $2m_e c^2 / \sin \theta$, where θ is the angle between the directions of the photon and the magnetic field, and the optical depth is given by

$$\tau_\gamma(\omega) = \frac{\alpha_f^2 h_\gamma}{2 r_e} B \sin \theta T(\chi); \quad 2/\sin \theta \leq \omega \quad (33)$$

where $\chi = \omega B \sin \theta / 2$ and

$$T(\chi) \approx \begin{cases} 0.46 \exp(-4/3x); & \chi \ll 1 \\ 0.6x^{-1/3}; & 1 \ll \chi \end{cases} \quad (34)$$

α_f is the fine structure constant; r_e is the classical electron radius; h_γ is the depth of the single-photon pair producing region; B is the magnetic flux density in units of the critical value $m_e^2 c^2 / \hbar e$ ($\approx 4.5 \times 10^9$ Tesla). Near threshold, $\omega = 2/\sin \theta$, the asymptotic expressions for $T(\chi)$ can overestimate the true value by several orders of magnitude (Daugherty & Harding 1983). For this process to be important for photons with energies in the MeV range the magnetic field strength has to have a magnitude approaching $m_e^2 c^2 / \hbar e$, a field strength generally only associated with neutron-star surfaces. For $\chi = 0.1$ the mean free path is $\sim 10^{-4} (B \sin \theta)^{-1}$ m and for $\chi = 0.05$ it is $\sim 10^2 (B \sin \theta)^{-1}$ m. The energy at which $\tau_\gamma = 1$ is very insensitive to h_γ ; we shall assume that it occurs at $\chi = 0.1$. The Thomson depth of the pairs is then

$$\tau_{es}^2 \approx 4x \frac{lh_\gamma}{R} \frac{1}{b\omega_M} \frac{2-\alpha}{\alpha-1} \left(\frac{\omega_M}{\omega_l} \right)^{\alpha-1} \quad (35)$$

where $\omega_l \approx \max(2, 0.2/B)$.

For small χ the pairs typically have an energy $\gamma \sim \omega/2$ when produced. As χ increases the energy is shared more unequally (Daugherty & Harding 1983). Since $B\omega/2 > 0.1$, most of the kinetic energy of the pairs is radiated as magnetic bremsstrahlung in the quantum regime (Erber 1966) where the spectrum peaks at $\omega \sim \gamma$. We therefore expect efficient conversion of energy into pairs, so x will take approximately its maximum value, giving

$$\tau_{es}^2 \approx \frac{2lh_\gamma}{bR} \quad (36)$$

We can see that, unlike the case of two-photon pair production, magnetic pair production can be optically thin to Thomson scattering, provided that $L < bR/2h_\gamma$. For a γ -ray burst with $L \sim L_{Edd}$ this requires $h_\gamma/R < 10^{-4}$. There is plenty of time for the pairs to cool before annihilating. The efficiency of the process means that, even for moderate τ_{es} a line feature could be observed.

6. Dynamics

6.1 Thermal Plasmas

The models we have considered so far have been static and so, in the absence of confinement, unphysical for low optical depths since the sound speed is greater than about $0.1 c$. The maximum time available before adiabatic cooling sets in and the proton Thomson depth begins to decrease is thus less than 10τ proton Thomson times. The low optical depth models would expand and cool adiabatically before much energy could be converted to radiation or

any pairs produced. For large τ , on the other hand, the cooling time is almost independent of τ . So all the thermal energy can be turned into radiation and pairs can be created and destroyed before the expansion is important. The photon escape time from the gas is proportional to τ^2 , however, and so for large τ the gas will expand before the radiation can escape.

Consider a sphere with an initial radius R_0 and Thomson depth τ_0 . The sound speed in the gas after cooling is

$$\beta_s \approx \left(\frac{kT_p^{init}}{m_p c^2} \right)^{1/2} \quad (37)$$

provided that $t_{cool} < R_0 / \beta_s c < \tau_0 R_0 / c$. Since $t_{cool} < R_0 / \beta_s c$, Comptonization of soft photons is no longer important by the time the gas starts to expand. The hard photons will have their energy reduced to $\omega_c \sim \beta_s \tau$, or a few times the electron temperature at $t = t_{cool}$, which ever is larger. Since $\tau_0 > 1 / \beta_s$ the photons are convected as the gas expands and only those at a radius greater than R_{esc} can escape, where

$$N_p \sigma_T (R - R_{esc}) = 1 / \beta_s \quad (38)$$

which gives

$$\xi_{esc} = \xi (1 - \xi^2 / \beta_s \tau_0); \quad \xi \equiv R / R_0 \quad (39)$$

We have assumed that the expansion speed is constant and equal to β_s , which is nearly true for $t > R_0 / \beta_s c$. As the gas expands the photons are cooled adiabatically, giving

$$\omega(\xi) = \omega(1) / \xi \quad (40)$$

The rate at which photons escape from the gas is

$$\text{rate} \propto \frac{d}{dt} \left(\frac{\xi_{esc}}{\xi} \right)^3 = \frac{6\xi}{\beta\tau_0} \left(1 - \frac{\xi^2}{\beta\tau_0} \right)^2 \frac{d\xi}{dt} \quad (41)$$

Let the spectrum of photons in the gas at $t = t_{cool}$ be

$$\text{spectrum} \propto \begin{cases} \omega^{-\alpha}; & \omega \leq \omega_c \\ 0; & \omega_c < \omega \end{cases} \quad (42)$$

Then the time integrated spectrum is

$$I(\omega) \propto \int_1^{\xi_{max}} \frac{6\xi}{\beta\tau_0} \left(1 - \frac{\xi^2}{\beta\tau_0} \right) \xi^{1-\alpha} \omega^{-\alpha} d\xi \quad (43)$$

where $\xi_{max} = \min \left[\omega_c / \omega, (\beta\tau_0)^{1/2} \right]$. Hence for $\omega > \omega_c / (\beta\tau_0)^{1/2}$ and $\alpha < 3$

$$I(\omega) \propto \omega^{-3} \quad (44)$$

and for $\omega < \omega_c / (\beta\tau_0)^{1/2}$ or $\alpha > 3$

$$I(\omega) \propto \omega^{-\alpha} \quad (45)$$

The computed spectra certainly have $\alpha < 3$, so the time-integrated spectra would have a break at $\omega \sim \omega_c / (\beta\tau_0)^{1/2}$ with the high-energy tail steepening to ω^{-3} . At energies $\omega > \omega_c$ the spectrum would be unaffected by the dynamics, since this part of the spectrum, not considered above, is dominated by pre-expansion emission at times $t < t_{cool}$.

6.2 Non-Thermal Plasmas

In order to produce an optically-thick pair plasma, the radiation energy density in the plasma is greater than $\tau_{pair} n_{pair} m_e c^2$, as we shall see, and hence the sound speed is approximately $c/\sqrt{3}$. The dynamical time is thus only slightly greater than a light-crossing time, and so the effect of radiation pressure will be important.

Consider a spherical region of radius R with Thomson depth $\tau_{pair} \gg 1$, in which uniformly distributed, fixed sources supply energy at a constant rate, \dot{e} , per unit volume. Since $\tau_{pair} \gg 1$ the radiation can be treated as a fluid on length scales greater than R/τ_{pair} . The time-independent equations governing the motion of the fluid are

$$(1-2u^2) \frac{de}{dr} = \frac{8eu^2}{r} - \frac{3eu}{c} \quad (46)$$

$$\frac{1-2u^2}{1+u^2} \frac{du}{dr} = \frac{3\dot{e}}{4ec} - \frac{2u}{r}$$

where $u = \gamma v/c$, v being the velocity; e is the energy density in the local rest frame of the fluid and we have assumed that the pressure is $e/3$ (see for example Landau & Lifshitz 1959). Solving for a as a function of u we obtain the familiar result

$$e = \frac{e_0}{(1+u^2)^2} = \frac{e_0}{\gamma^4} \quad (47)$$

where $e_0 \equiv e(r=0)$.

With the use of this result we find, after some algebra,

$$\frac{v}{\gamma^2} = \frac{3\dot{e}}{4e_0} \frac{1}{r^2} \int_0^r \gamma r_1^2 dr_1; \quad \dot{e} \neq 0, r \leq R \quad (48)$$

$$\frac{v}{\gamma^2} \propto \frac{1}{r^2}; \quad \dot{e} = 0, R < r$$

Now v/γ^2 has a maximum at $v = c/\sqrt{3}$, whereas the right-hand side of the above equations are monotonic functions of r . The only solution with $de/dr < 0$ for $r > R$ is the one for which $v = c/\sqrt{3}$ at $r = R$. Putting $x = r/R$ we have

$$\frac{v}{\gamma^2} = \frac{\dot{e}R}{4e_0} x \left[1 + \frac{3}{x^3} \int_0^x \frac{u^2}{1+\gamma} x_1^2 dx_1 \right]; \quad x \leq 1 \quad (49)$$

$$\frac{v}{\gamma^2} = \frac{2}{3\sqrt{3}} \frac{1}{x^2}$$

where e_0 is fixed by the condition on the solution at $x = 1$. This solution is continuous, but not differentiable, at $x = 1$. Now $d^2u/dx^2 > 0$ for $0 \leq x < 1$ and so $u \leq x/\sqrt{2}$ for $0 \leq x < 1$, giving

$$\int_0^1 \frac{u^2}{1+\gamma} x^2 dx < \frac{1}{4} \int_0^1 x^4 dx = \frac{1}{20} \quad (50)$$

Hence

$$\frac{3\sqrt{3}}{8} \frac{\dot{e}R}{c} < e_0 < \frac{23}{20} \frac{3\sqrt{3}}{8} \frac{\dot{e}R}{c} \quad (51)$$

for $r < R$, $v \propto r$, which gives

$$n(r < R) \sim \text{const} \sim \left(\frac{f\dot{e}}{b\sigma_T m_e c^3} \right)^{1/2} \quad (52)$$

where $f(\leq 1)$ is the fraction of \dot{e} which is converted into pairs and n is the density of electrons plus positrons. If L is the source luminosity then

$$\dot{e} = \frac{3}{4\pi R^3} L = \frac{3lm_e c^2}{4\pi R^2 \sigma_T} \quad (53)$$

and hence

$$\tau \equiv n\sigma_T R = \left(\frac{3fl}{4\pi b} \right)^{1/2} \quad (54)$$

and so $\tau \gg 1$ requires

$$l \gg 4\pi b/3f \quad (55)$$

The same result is obtained by Guilbert, Fabian & Rees (1983) ignoring motion in the source. This is to be expected since for $\tau \gg 1$ the pair production and annihilation time-scales are $R/\tau c \ll R/c$. The ratio of the radiation energy density e_0 to $nm_e c^2$ is

$$\frac{e_0}{nm_e c^2} \approx \frac{9}{8\sqrt{3}} \frac{b\tau}{f} \gg 1 \quad (56)$$

justifying our initial assumption that the radiation energy density is much greater than $nm_e c^2$. For $r > R$ we have

$$\frac{1}{r^2} \frac{d}{dr} (nr^2 v) = -\frac{n^2}{\gamma^2} b\sigma_T c \quad (57)$$

where n is measured in the rest frame of the source. Since for $r > R$, $v > c/\sqrt{3}$ and $\gamma^2 \propto vr^2$ we shall assume $v = c$, giving

$$\tau\gamma = \tau_R \gamma_R / \left[1 + \frac{b\tau_R \gamma_R}{3} \left(\frac{1}{\gamma_R^3} - \frac{1}{\gamma^3} \right) \right] \quad (58)$$

where $\tau = n\sigma_T r$ and subscript R indicates that the value of the quantity at $r = R$ is to be taken. If the only coupling between the radiation and the pairs is Compton scattering then the maximum value of γ is

$$\gamma_{\max}^3 \sim \tau_R \gamma_R / \left(1 + \frac{b\tau_R}{3\gamma_R^2} \right) \quad (59)$$

(The fluid approximation breaks down at $\tau \sim \gamma^2$). In the limit of large τ_R this gives

$$\gamma_{\max} \sim \gamma_R (3/b)^{1/3} \quad (60)$$

The pairs will be cold, $kT_{\text{pair}} \ll m_e c^2$ (see Guilbert, Fabian & Rees 1983) and hence $b \sim 1/2$, giving

$$\gamma_{\max} \sim 2 \quad (61)$$

In this case only a mildly relativistic wind will be produced. If the pair production process is inefficient, $f \ll 1$, then a large fraction of the kinetic energy of the pairs that are produced must be radiated as soft photons. In this case the free-free and cyclotron absorption cross-sections may be more relevant than the Thomson cross-section.

Outside the source, in the wind where pairs are no longer being produced, self-absorption may still be important if, for instance, a small magnetic field is carried along with the pairs. The hard photons, in particular the annihilation photons produced in the wind, will escape when $\gamma > 2$. However, if even a small fraction of the radiation is still trapped it can drive the wind to a much larger γ .

Assuming that all the radiation escapes at $\gamma = 2$ then the fraction of the total luminosity carried away by the pairs is

$$\frac{L_{pair}}{L} \sim \frac{4}{l} \quad (61)$$

So even if pair production is very efficient, nearly all the energy is carried away by the radiation. The spectrum will be significantly affected by the dynamics of the wind since photons are convected and therefore scatter much less, $\propto \tau_R$ times instead of $\propto \tau_R^2$ times. In particular the hardest photons to escape will be those produced by pair annihilation in the wind. (Note that the energy flux in pairs at the base of the wind $\sim L\tau_R/l$). These annihilation photons will be blueshifted to a maximum energy of $(1 + \beta_{max})\gamma_{max} \sim 4$ and Compton-scattered to give a flat component to the spectrum with a turnover at ~ 2 MeV. The low energy part of the spectrum has been discussed in Guilbert, Fabian & Rees (1983), although no account was taken of the reduction in the photon-electron coupling due to motion and the blueshifting of the observed photons.

7. Conclusions

We have considered electron-positron pair production in thermal plasmas of moderate depth to Thomson scattering and found that pairs are either unimportant, $z < z_{crit} \sim 0.1$, or else pair production runs away. This result is independent of the thermal assumption; it is due to the non-linearity of the system. A similar result is found for any plasma where the pairs themselves produce and scatter photons to energies capable of making more pairs. Mathematically this can be seen by inspection of equation (13). It is the parameter a which contains all the physical details of the photon production and pair annihilation cross-sections. The only change in the structure of the equation in the non-thermal case is the change to a linear dependence on $1 + 2z$ (the total number of electrons and positrons per proton) in the photon production rate. This increases z_{crit} to approximately 0.2. Physically, we can see that $z < 1$ for stability. At $z \sim 1$ the photon production rate becomes proportional to z (z^2 in the thermal case) but the escape rate is constant. In any system where $z \gtrsim 1$, therefore, a slight increase in z implies the creation of more photons capable of producing even more pairs, so z increases and the pair density runs away.

The region of parameter space in the T, τ_p plane where equilibrium solutions are possible is given by an equation like (14) and depends sensitively on all the physics as well as the geometry of the gas. For thermal gases, however, Thomson depths greater than a few are unstable to runaway pair production when the temperature is greater than 100–200 keV.

For the time-dependent case we obtained a system of four ordinary differential equations, (17)–(20), governing the behaviour of the electron and proton temperatures and the pair density as a function of time. Solving these showed that about 10 proton Thomson times are required to reach z_{max} . The greater the initial heating (i.e. the larger T_p^{init}) the greater z_{max} and the lower the final electron temperature. Most of the cooling takes place when $z \sim z_{max}$. Since T_e reaches nearly its final value at $z = z_{max}$, the more heat added to the gas initially, the cooler the resulting radiation. This result had also been obtained implicitly for nonthermal pair production by Guilbert, Fabian & Rees (1983). It will always be true if the photon

number density is dominated by photons with less than the average electron energy, since the photon-electron coupling increases exponentially with z through Compton scattering.

The detailed numerical models described in Section 4 give more accurate results for gases with plane geometry and also provide the radiation spectrum. We can see (fig. 8 and 10) that the spectra produced by these models are too hard to represent, for example, observed active galactic nuclei. In particular the very flat part of the spectrum between ~ 20 – 200 keV, due to Compton-scattered annihilation photons, is harder than anything observed in that energy range, even from γ -ray bursters, as far as we are aware.

Proton temperatures needed to drive the electron temperatures into the unstable regime of runaway pair production imply dynamical times of the order of 10τ proton Thomson times. The static models summarized above are in general unphysical, unless there is some confinement. Note that non-thermal heating does not solve this problem. At $z = z_{max}$, $T_e < 1$ and so only an exponentially small fraction of the total energy is in pairs. Hence $(P_{rad} / \rho_{gas})^{1/2} > 1/30$ for $z_{max} > 1$. Magnetic fields on the surface of neutron stars are, in principle, easily capable of confining a pair-dominated plasma and also capable of inducing single-photon pair production. If magnetic pair production dominates ordinary two-photon pair production then the plasma can still be optically thin to Thomson scattering, *even if all the γ -ray flux above 1 MeV is turned into pairs*. In this case Comptonization will not necessarily flatten the spectrum. In particular it allows the annihilation photons to escape as a line rather than as the broad flat component seen in Fig. (10).

Finally we considered the effect of free expansion in two special cases. In the thermal case of large τ the result is that the hard, flat annihilation plateau in the spectrum would never appear but would be a steep ω^{-3} power law. In the very idealized non-thermal case the spectrum has not been calculated. However, the dynamics significantly affect the radiation transport by greatly reducing the time a photon spends in the gas. A pair wind is produced with a maximum $\gamma \sim 2$, resulting in a spectral turnover at ~ 2 MeV due to annihilation of pairs in the wind.

Acknowledgments

Part of this work was completed while PWG was at JILA. The computations in this paper were carried out on the CRAYs at NCAR (Colorado) and Max-Planck, the IBM 3081 at Cambridge, and a BBC micro. We thank Martin Rees for helpful discussions on the dynamics sections, and Roland Svensson for a critical reading of the manuscript. SS thanks SERC and Newnham College for support.

References

- Bisnovatyi-Kogan, G. S., Zel'dovich, Ya. B. & Syunyaev, R. A., 1971. *Soviet Astr.*, **15**, 17.
Bussard, R. W., Ramaty, R. & Drachman, R. S., 1979. *Astrophys. J.*, **228**, 928.
Daugherty, J. K. & Harding, A. K., 1983. *Astrophys. J.*, **273**, 761.
Erber, T., 1966. *Rev. Mod. Phys.*, **38**, 626.
Guilbert, P. W., 1981a. *Mon. Not. R. astr. Soc.*, **197**, 451.
Guilbert, P. W., 1981b. *Ph.D. thesis*, University of Cambridge.
Guilbert, P. W., Fabian, A. C. & Rees, M. J., 1983. *Mon. Not. R. astr. Soc.*, **205**, 593.
Guilbert, P. W., Fabian, A. C. & Stepney, S., 1982. *Mon. Not. R. astr. Soc.*, **199**, 19P.
Johnson, W. N. III, Harnden, P. R. Jr & Haymes, R. C., 1972. *Astrophys. J.*, **172**, L1.
Landau, L. D. & Lifschitz, E. M., 1959. *Fluid Mechanics*, Pergamon Press, Oxford.
Leventhal, M., MaeCullam, C. J. & Stang, P. D., 1978. *Astrophys. J.*, **225**, L11.
Lightman, A. P., 1982. *Astrophys. J.*, **253**, 842.
Lightman, A. P. & Band, D. L., 1981. *Astrophys. J.*, **251**, 713.

- Mazets, E. P. *et al.* 1981. *Astrophys. Space Sci.*, **88**, 3.
- Nolan, P. L. & Matteson, J. L., 1983. *Astrophys. J.*, **265**, 389.
- Stepney, S., 1983a. *Mon. Not. R. astr. Soc.*, **202**, 467.
- Stepney, S., 1983b. *Ph.D. thesis*, Cambridge University.
- Stepney, S. & Guilbert, P. W., 1983. *Mon. Not. R. astr. Soc.*, **204**, 1269.
- Svensson, R., 1982. *Astrophys. J.*, **258**, 335.
- Svensson, R., 1984. *Mon. Not. R. astr. Soc.*, **209**, 175.
- Zdziarski, A. A., 1982. *Astr. Astrophys.*, **110**, L7.
- Zdziarski, A. A., 1984a. *Phys. Scripta*, **T7**, 124.
- Zdziarski, A. A., 1984b. *Astrophys. J.*, **283**, in press.